SI Appendix

SI Text 1. *Calculation of toxic concentrations of digitoxin from published blood levels in patients.* Goodman and Gillman (1) indicate that digitoxin toxicity can begin at concentrations greater than ≈30 ng/ml (or ≈40 nM). Smith (2) summarized a large amount of individual reports on digitoxin levels measured in patients either with or without toxicity. The average digitoxin concentration in patients without toxicity, based on reports from ten different authors, was 21.7 ng/ml (n = 10) or ≈31 nM. By contrast, the average digitoxin concentration in patients with toxicity, based on reports from eight different authors, was 32.75 ng/ml (n = 8) or ≈43 nM. This value is very close to the 40 nM (namely, ≈30 ng/ml) value stated in Goodman and Gillman (1) for the beginning of toxicity. Explicitly, we calculated the molar equivalent of 30 ng/ml by dividing the g/liter value by the molecular weight of digitoxin (namely, 764 g/mole).

1. Roden DM (1996) in *Goodman and Gilman's The Pharmacological Basis of Therapeutics*, eds Hardman JG, *et al*. (McGraw--Hill, New York), 9th Ed, p 864.

2. Smith, TW (1975) Digitalis toxicity: Epidemiology and clinical use of serum concentration measurements. *Amer J Med* 58:470-476.\

Figure Legends

Fig. 5. Kinetics for digitoxin-dependent changes in intracellular calcium concentration. (*a*) Rates of change of calcium concentration in the presence of 80 nM digitoxin. PC12 cells were loaded with FURA-2AM, as described in Methods, and 50 cells optically marked for simultaneous analysis of intracellular calcium concentration. Digitoxin, at a concentration of 80 nM, was added, and the signals followed over a ten minute time period. In the example shown, 74% of the cells responded, of which several traces have been abstracted from the entire dataset for display. Three independent experiments were performed with similar results. (*b*) Effect of extracellular EGTA in digitoxin-induced calcium uptake. PC12 cells were loaded with FURA-2AM, as described in Methods, and

50 cells optically marked for simultaneous analysis of intracellular calcium concentration. Cells were studied in a calcium free media containing EGTA (2 mM), and 80 nM digitoxin then added. The trace shown is representative of the entire set of cells. Three independent experiments were performed with similar results. (*c*) Effect of anti-digitoxin antibody on digitoxin induced change in intracellular calcium concentration. PC12 cells were loaded with FURA-2AM, as described in *Methods*, and 50 cells optically marked for simultaneous analysis of intracellular calcium concentration. Monoclonal anti-digitoxin antibody was added to the culture, followed immediately by 80 nM digitoxin. Three independent experiments were performed with similar results.

Fig. 6. Influence of digitoxin on cytotoxicity and cell survival. PC12 cells were incubated in different concentrations of digitoxin for three days, washed, and assayed for released LDH. (*Inset*) Cells incubated in parallel were assayed for XTT activity. Open circles, incubated in serum-free medium; filled circles, incubated in 10% serum-containing (FBS) medium.

Fig. 7. PC12 cells expressing high levels of extracellular PS are exhibit higher cytotoxicity to digitoxin. (*a*) FACS analysis of PS-positive and PS-negative subclones of PC12 cells in pure PC12 culture. (*Left*) Unlabeled PC12 cells enter the cell sorter and emerge as a single peak. These are labeled "C." Since these are unlabeled cells, there is no fluorescent signal in the distal box. (*Right*) The PC12 cells are labeled with AnnexinV-FITC and sorted. Cells emerge as two peaks. "A"s are PS negative (-) cells. "B"s are PS positive (+) cells. (*b*) XTT-measures cell death after 24 hours in culture in digitoxin (10, 100 and 500 nM). PS (+) cells are significantly more sensitive than PS(-) cells to all digitoxin concentrations. P values are indicated by asterisks. Control cultures ("C"), which are mixtures of PS(+) and PS(-) cells, give intermediate values. (*c*) LDH release measures cytotoxicity after 24 hours in culture in digitoxin (10, 100, and 500 nM). PS (+) cells are significantly more sensitive than PS(-) cells to all digitoxin concentrations. P values are indicated by asterisks. Control cultures ("C"), which are mixtures of PS(+) and PS(-) cells, give intermediate values.

Fig. 8. Antibody against digitoxin blocks digitoxin channels in neutral (POPC/POPE) planar lipid bilayer. (*a*) Influence of anti-digitoxin antibody on digoxin channels in neutral planar lipid bilayer. (*Top*) The "before" record illustrates the current activity observed at zero and at 10 mV bilayer electrical potential difference prior to addition of the Clone DI-22 antibody. (*Middle*) The "after 10 min" record illustrates the current activity observed at zero and at 10 mV bilayer electrical potential difference ten minutes after addition of the Clone DI-22 antibody. (*Bottom*) The "after 14 min" record illustrates the current activity observed at zero and at 10 mV bilayer electrical potential difference fourteen minutes after addition of the Clone DI-22 antibody. The currents in the latter condition are nearly zero, and the openings are quite long. (*b*) Amplitude histogram of digitoxin channels at different intervals after addition of anti-digitoxin antibody. Gaussian fits to the channels amplitudes and respective frequencies, as a function of antibody exposure time are shown as histograms. (*c*) Current-voltage curves for antibody-dependent conductance changes for digitoxin channels over time. The digitoxin channels begin at 75 pS. By 10 minutes, the conductance is 45 pS. By 14 minutes, the conductance is 22 pS. The curve intercepts generate an average equilibrium potential of 24.63 ± 0.62 mV.

Fig. 9. Lanthanum chloride inhibits digitoxin channels. (*a*) Traces of digitoxin channel activity in POPS/POPE planar lipid bilayer before and after addition of $LaCl_3$. Uppermost trace shows that a digitoxin channel is established in a gradient of CsCl, just as shown for Fig. 2*a*. The digitoxin is added to the 200 mM CsCl chamber at a final concentration of 43 μM. The two middle traces show digitoxin channel activity after sequential elapsed times of 20 seconds in 8.33 μM $LaCl_3$, and after 54 seconds in 16.66 μM $LaCl_3$, respectively. The bottom trace shows digitoxin channel activity after a sequential elapsed time of one minute, after washing the 200 mM CsCl/digitoxin chamber with fresh 200 mM CsCl buffer. (*b*) Current amplitude histogram of digitoxin channel activity after each step in treatment with $LaCl_3$, as shown in *a*. The current amplitude histogram shows the distribution of the current events from a representative sixty seconds current segment taken at zero bilayer potential. The histogram was fitted to a multi-Gaussian function.

Fig. 10. Aluminium chloride inhibits digitoxin channels. (*a*) Traces of digitoxin channel activity in POPS/POPE planar lipid bilayer before and after addition of $AlCl_3$. *Top Trace*: A digitoxin channel is established in a gradient of CsCl, just as shown for Figure 2a. The digitoxin is added to the 200 mM CsCl chamber at a final concentration of 43 μM. *Trace #2:* Digitoxin channels are shown after a sequential elapsed time of 1.33 minutes in 8.33 μM $AlCl_3$. *Trace #3*: Digitoxin channel activity is shown at a sequential elapsed time of 2.43 minutes after increasing the $AlCl_3$ concentration in the chamber to 16.66 μM. *Trace #4*: Digitoxin channels are shown after a sequential elapsed time of 1.31 minutes, after increasing the $AlCl_3$ concentration in the chamber to 25 μM. (*b*) Current amplitude histogram of digitoxin channels activity after each step in treatment with $AlCl_3$, as shown in part *a*. The current amplitude histogram shows the distribution of the current events from a representative sixty seconds current segment taken at zero bilayer potential. The histogram was fitted to a multi-Gaussian function.

Fig. 11. Magnesium chloride fails to inhibit digitoxin channel activity. (*a*) Traces of digitoxin channel activity in POPE/POPS planar lipid bilayer before and after addition of $MgCl_2$. *Top Trace*: A digitoxin channel is established in a gradient of CsCl, just as shown for Figure 2a. The digitoxin is added to the 200 mM CsCl chamber at a final concentration of 43 μM. *Trace # 2:* Digitoxin channels are shown after elapsed times of 1.34 minutes in 16.66 μM $MgCl_2$. *Trace #3*: Digitoxin channels are shown after elapsed times of 42.93 seconds, after increasing the $MgCl_2$ concentration in the chamber to 33.32 μM. *Trace #4* (*bottom*): Digitoxin channels are shown after elapsed times of 36.3 seconds, following addition of 60 μM $LaCl_3$. (*b*) Current amplitude histogram of digitoxin channel activity after each step in treatment with $MgCl_2$, as shown in part *a*. The current amplitude histogram shows the distribution of the current events from a representative sixty seconds current segment taken at zero bilayer potential. The histogram was fitted to a multi-Gaussian function.

Fig. 12. Nitrendipine fails to inhibit digitoxin channels. (*a*) Traces of digitoxin channel activity in POPE/POPS planar lipid bilayer before and after addition of nitrendipine. *Top Trace*: A digitoxin channel is established in a gradient of CsCl, just as shown for Figure

2a. The digitoxin is added to the 200 mM CsCl chamber at a final concentration of 43 μM. *Trace # 2:* Digitoxin channel activity is shown after elapsed times of 50.2 seconds in 16.66 μM nitrendipine. *Trace #3*: Digitoxin channel activity is shown after elapsed times of 40 seconds, after increasing the nitrendipine concentration in the chamber to 33.32 μM. *Trace #4(bottom)*: Digitoxin channels are shown after elapsed times of 1.01 minute, following addition of 60 μM $LaCl_3$. (*b*) Current amplitude histogram of digitoxin channels after each step in treatment with nitrendipine, as shown in part *a*. The current amplitude histogram shows the distribution of the current events from a representative sixty seconds current segment taken at zero bilayer potential. The histogram was fitted to a multi-Gaussian function.

Fig. 13. Structures and activities of digitoxin-related cardiac glycosides. (*a*) Oleandrin forms digitoxin-like cation-specific channels in POPS/POPE planar lipid bilayers. The structure of oleandrin is shown in the upper panel, and the channel activity shown in the lower panel. All conditions are as described for digitoxin channels in Figure 2. A continuous recording of 12 seconds is shown. The concentration of oleandrin is 43 nM. These data are representative of three independent experiments. (*b*) Digoxin forms digitoxin-like cation-specific channels in POPS/POPE planar lipid bilayers. The structure of digitoxin is shown in the upper panel, and the channel activity shown in the lower panel. All conditions are as described for digitoxin channels in Fig. 2. A continuous recording of 12 seconds is shown. The concentration of digoxin is 43 nM. These data are representative of three independent experiments. (*c*) Digoxigenin 3,12-diAc forms digitoxin-like cation-specific channels in POPS/POPE planar lipid bilayers. The structure of digoxigenin 3, 12-diAc is shown in the upper panel, and the channel activity shown in the lower panel. All conditions are as described for digitoxin channels in Fig. 2. A continuous recording of 12 seconds is shown. The concentration of digoxigenin 3, 12-diAc is 43 nM. These data are representative of three independent experiments.

Fig. 14. Summary of concentration dependent actions of digitoxin. (1) In concentration range of 0.1-2.0 nM, digitoxin blocks the interaction between TNFR1 and TRADD, and

downstream expression of IL-8. (2) The therapeutic window for heart failure is *ca.* 5-30 nM. (3) In range of 10-100 nM, digitoxin blocks hERG channels. (4) Above ca. 40 nM, digitoxin forms multimeric calcium channels. (5) In range of 300 nM and above, digitoxin and other active cardiac glycosides block the NaKATPase. (6) In range of 3-20 μM, active cardiac glycosides block the Na^{+}/ Ca^{++} Exhanger (NCX) via action on the NaKATPase. Colored arrows discriminate between the three discrete clusters of functional activities.

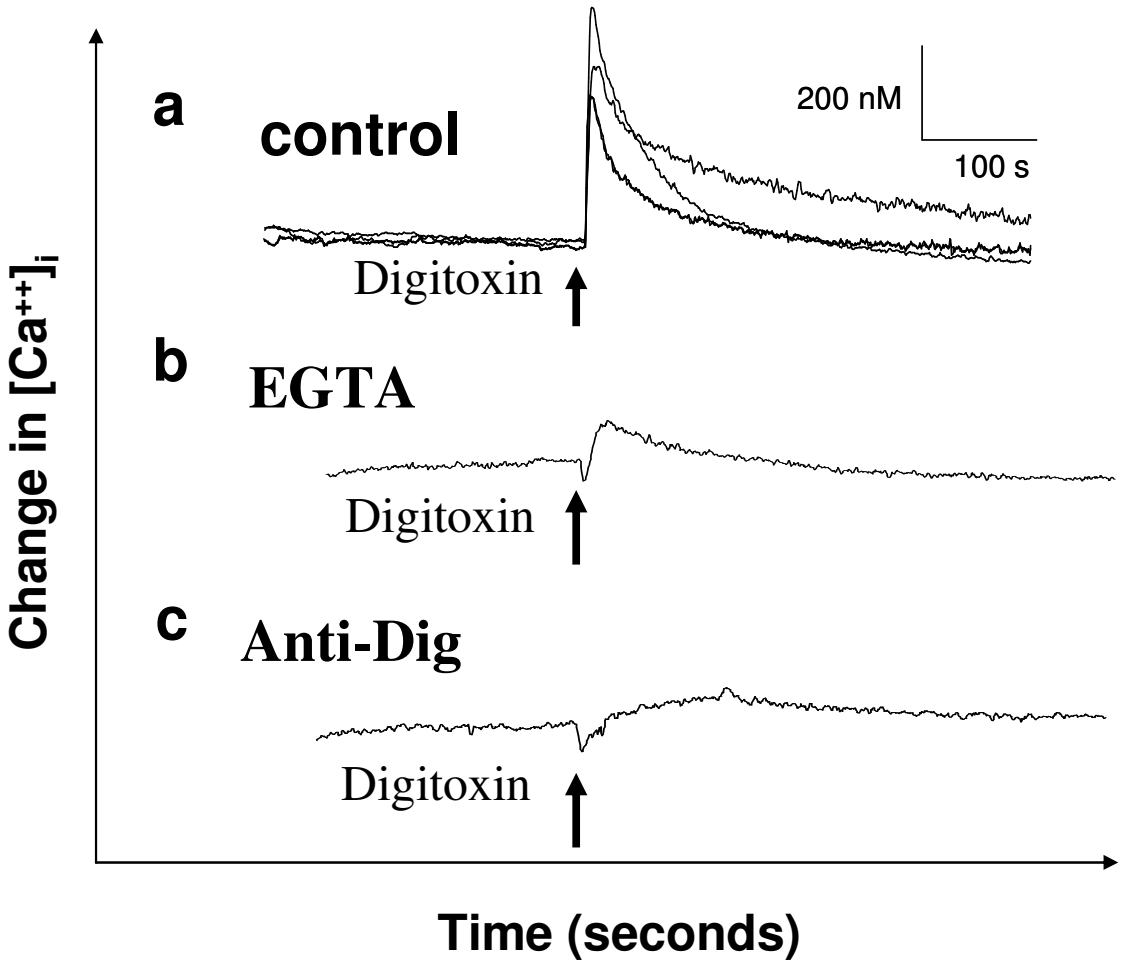
a
control
200 nM
100 s
Digitoxin
b
EGTA
Digitoxin
c
Anti-Dig
Digitoxin
Change in [Ca++]i
Time (seconds)

1S

Supplemental Figure 5. Kinetics for digitoxin-dependent changes in calcium concentration

a. Rates of change of calcium concentration in the presence of 80 nM digitoxin

b. Effect of extracellular EGTA in digitoxin-induced calcium uptake.

c. Effect of anti-digitoxin antibody on digitoxin induced change in intracellular calcium concentration.

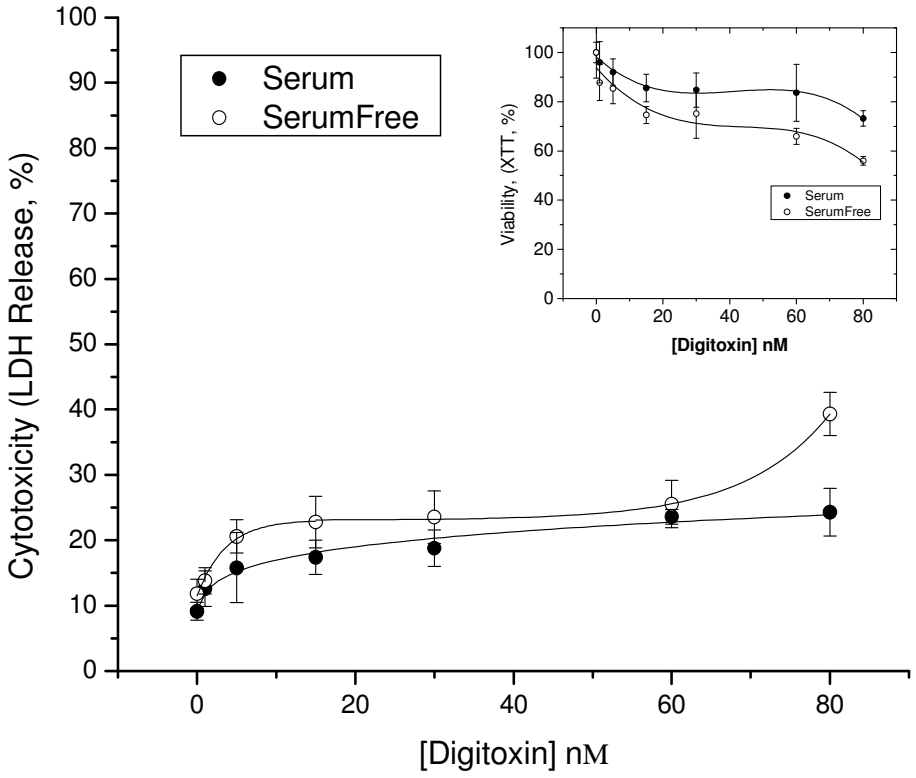
Cytotoxicity (LDH Release, %)
[Digitoxin] nM
Serum
SerumFree
Viability, (XTT, %)
[Digitoxin] nM
Serum
SerumFree

2S

Supplemental Figure 6. Influence of digitoxin on cytotoxicity (%LDH release) and cell survival (%XTT, inset).

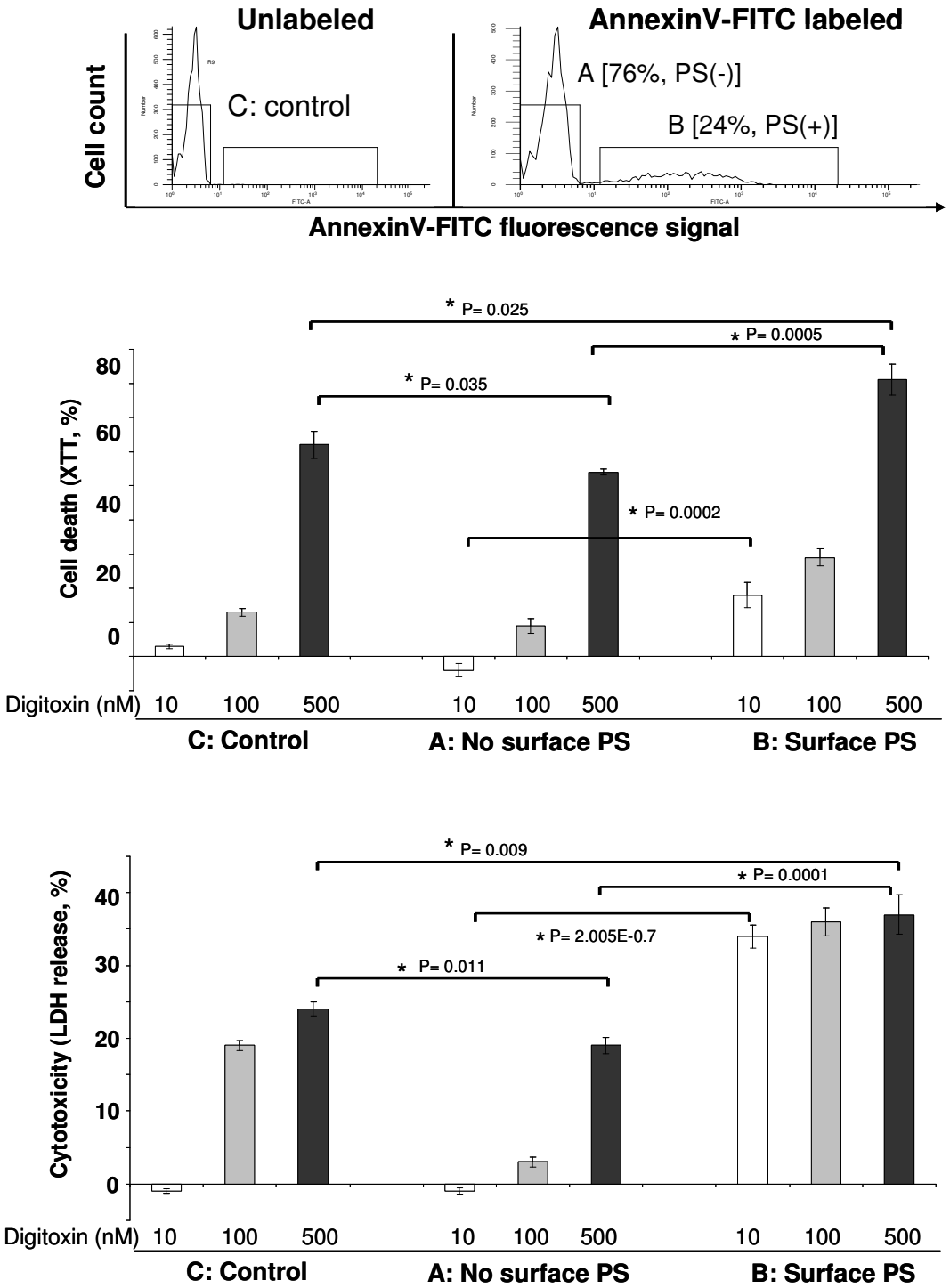

SupFig. 7. PC12 cells expressing high levels of extracellular PS are exhibit higher cytotoxicity to digitoxin.

(*a*) FACS analysis of PS-positive and PS-negative subclones of PC12 cells in pure PC12 culture. "C" are total cells. "A" are PS-negative, and B are "PS-positive subclones. (*b*) XTT-measures of cytotoxicity after

24 hours in culture in digitoxin (10, 100, and 500 nM). (*c*) LDH release measures of cytotoxicity after 24 hours in culture in digitoxin (10, 100, and 500 nM).

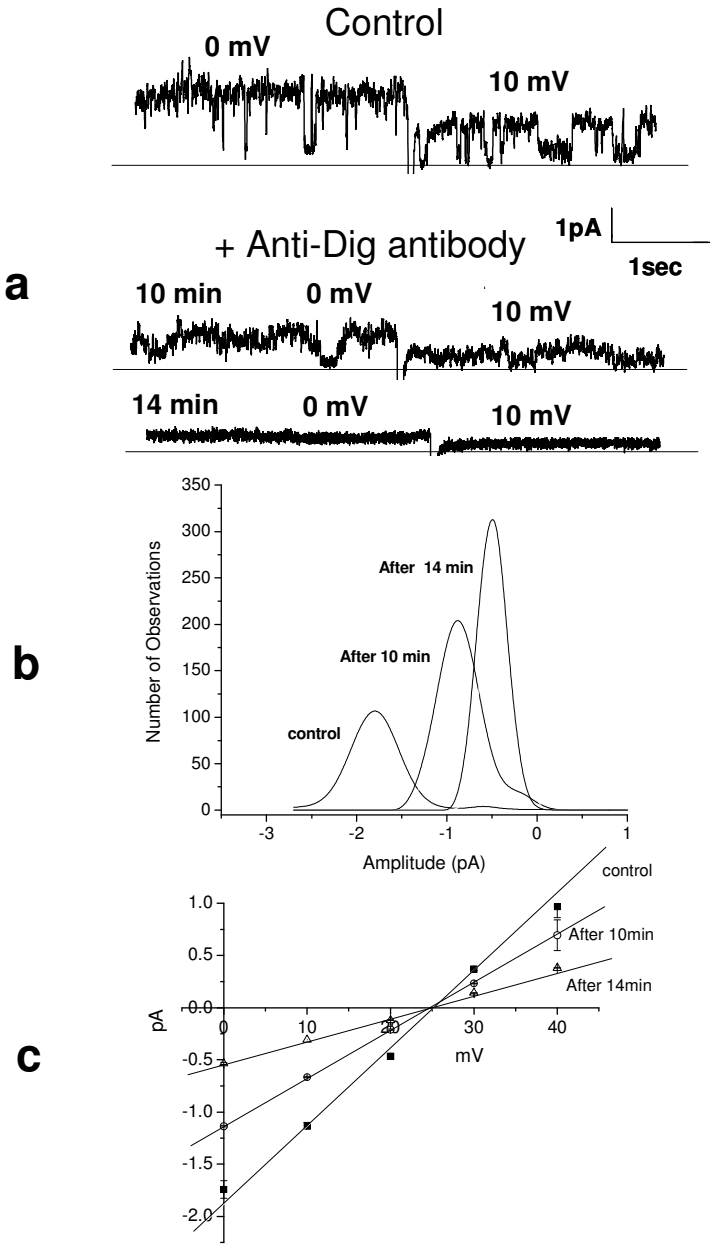

3S

Fig. 8. Antibody against digitoxin blocks digitoxin channels in neutral planar lipid bilayer. (*a*) Influence of anti-digitoxin antibody on digoxin channels in neutral planar lipid bilayer. Upper record: (*b*) Amplitude histogram of digitoxin channels at different intervals after addition of anti-digitoxin antibody. (*c*) Current-voltage curves for antibody-dependent conductance changes for digitoxin channels over time.

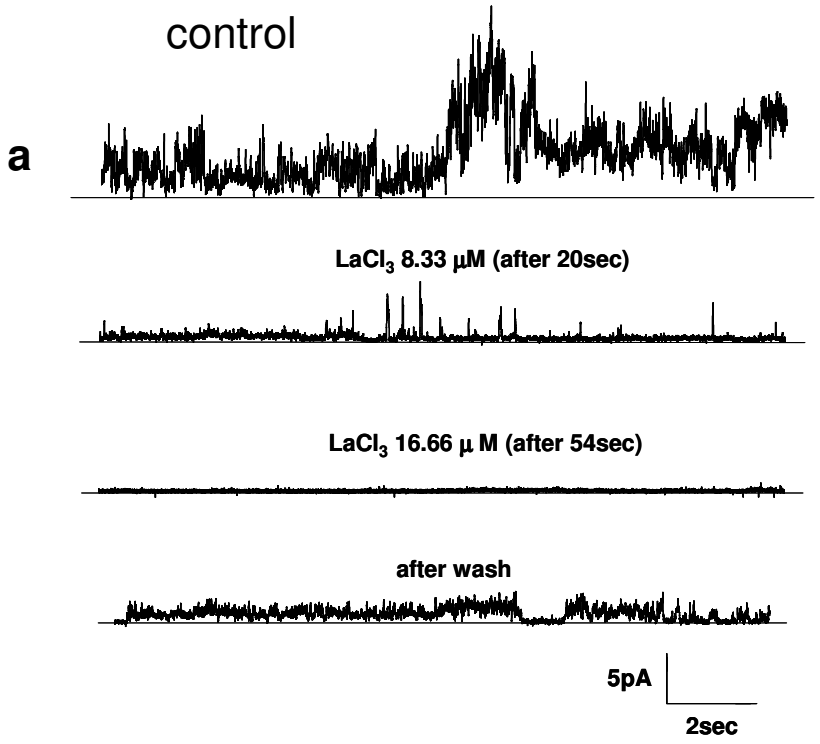
a
control
LaCl3 8.33 µM (after 20sec)
LaCl3 16.66 µ M (after 54sec)
after wash
5pA
2sec

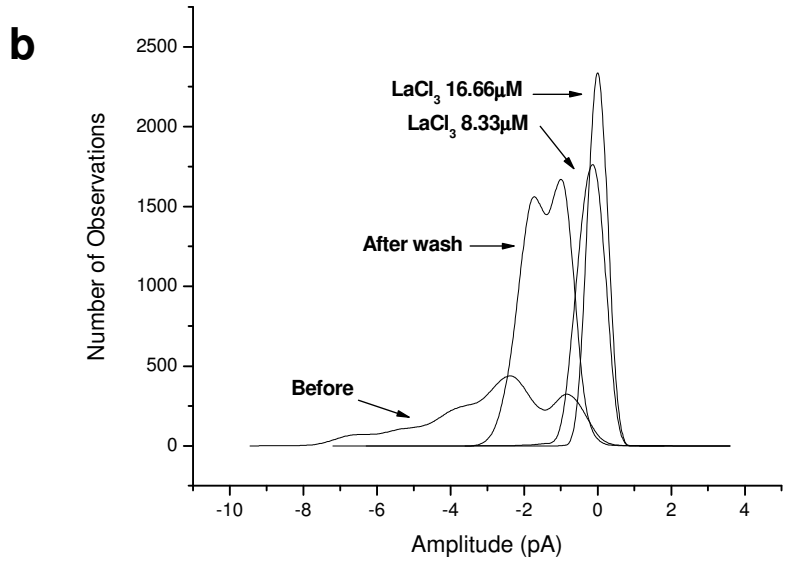
b
Number of Observations
2500
2000
1500
1000
500
0
LaCl3 16.66µM
LaCl3 8.33µM
After wash
Before
-10
-8
-6
-4
-2
0
2
4
Amplitude (pA)

5S

Fig. 9. Lanthanum chloride inhibits digitoxin channels. (*a*) Traces of digitoxin channels activity in POPS/ POPE planar lipid bilayer before and after addition of $LaCl_3$. (*b*) Current amplitude histogram of digitoxin channels after each step in treatment with $LaCl_3$, as shown in *a*.

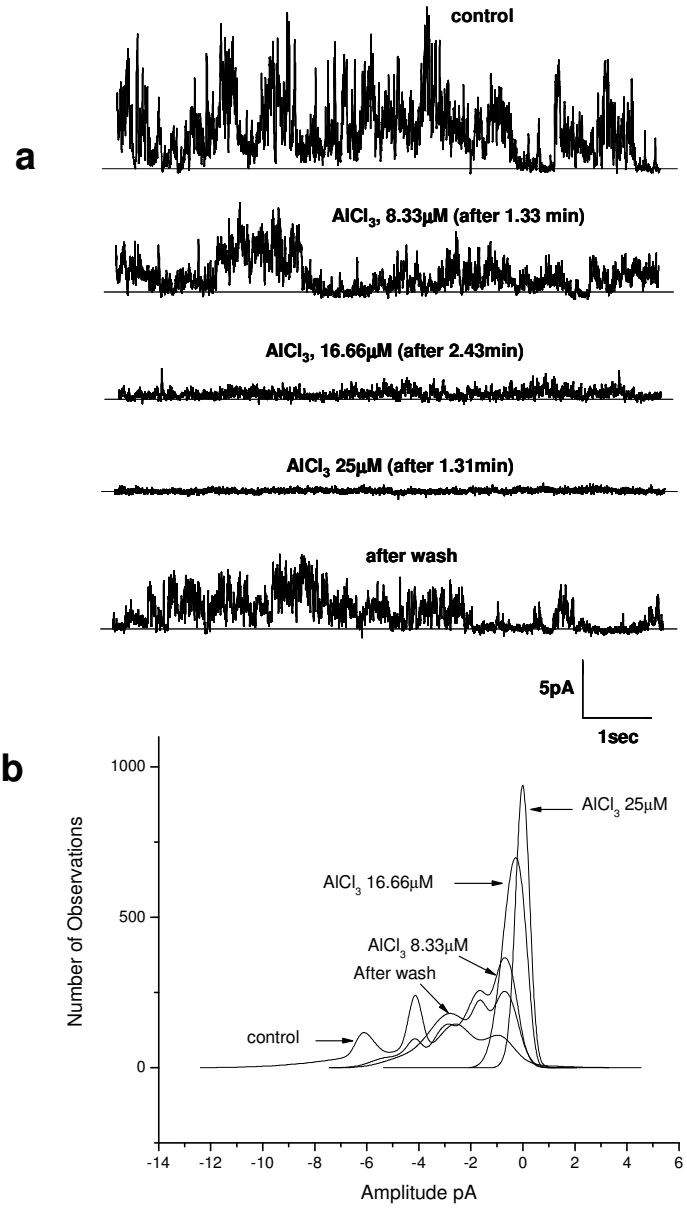

Fig. 10. Aluminium chloride inhibits digitoxin channels. (*a*) Traces of digitoxin channels activity in POPS/ POPE planar lipid bilayer before and after addition of $AlCl_3$. (*b*) Current amplitude histogram of digitoxin channels after each step in treatment with $AlCl_3$, as shown in *a*.

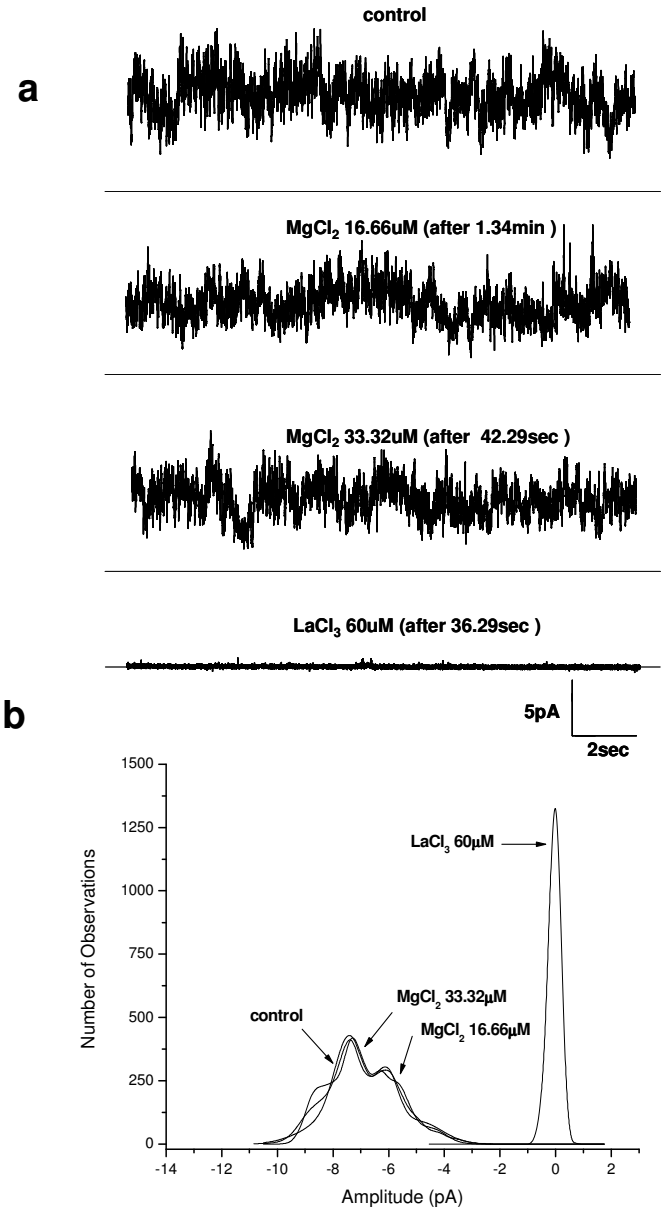
a
control
MgCl2 16.66uM (after 1.34min)
MgCl2 33.32uM (after 42.29sec)
LaCl3 60uM (after 36.29sec)
5pA
2sec
b
Number of Observations
Amplitude (pA)
LaCl3 60μM
MgCl2 33.32μM
MgCl2 16.66μM
control
1500
1250
1000
750
500
250
0
-14
-12
-10
-8
-6
-4
-2
0
2

Fig. 11. Magnesium chloride fails to inhibit digitoxin channels. (*a*) Traces of digitoxin channels activity in POPS/ POPE planar lipid bilayer before and after addition of $MgCl_2$. (*b*) Current amplitude histogram of digitoxin channels after each step in treatment with $MgCl_2$, as shown in *a*.

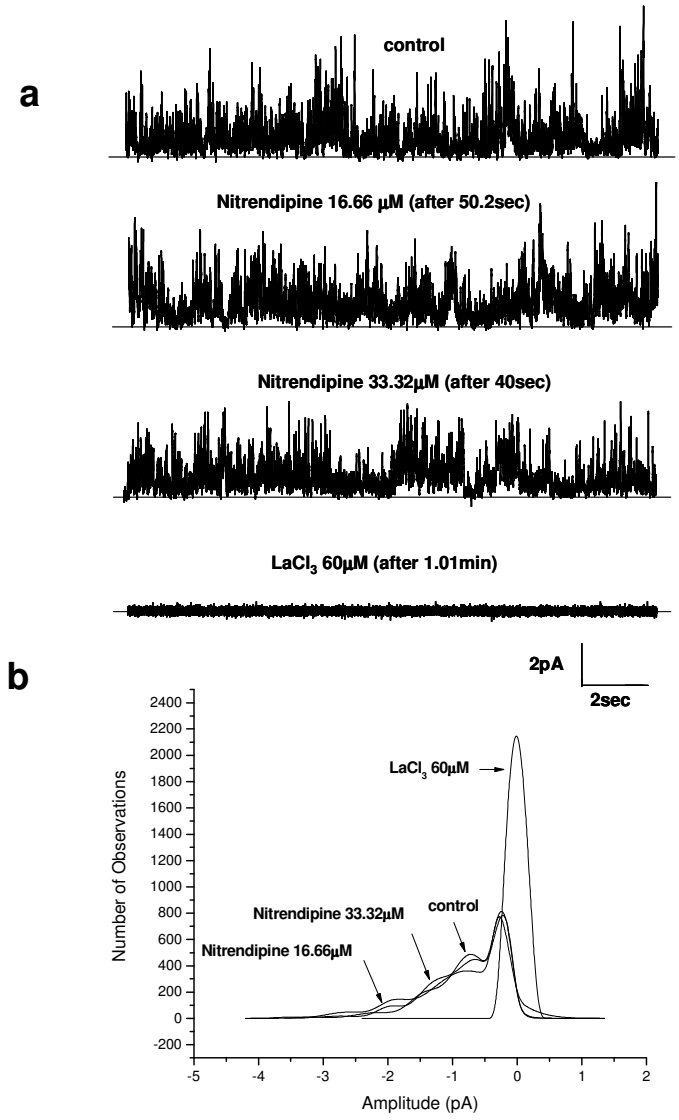
a
control
Nitrendipine 16.66 µM (after 50.2sec)
Nitrendipine 33.32µM (after 40sec)
LaCl3 60µM (after 1.01min)
b
2pA
2sec
LaCl3 60µM
Nitrendipine 33.32µM
control
Nitrendipine 16.66µM
Number of Observations
Amplitude (pA)

Fig. 12. Nitrendipine fails to inhibit digitoxin channels. (*a*) Traces of digitoxin channels activity in POPS/ POPE planar lipid bilayer before and after addition of nitrendipine. (*b*) Current amplitude histogram of digitoxin channels after each step in treatment with nitrendipine, as shown in *a*.

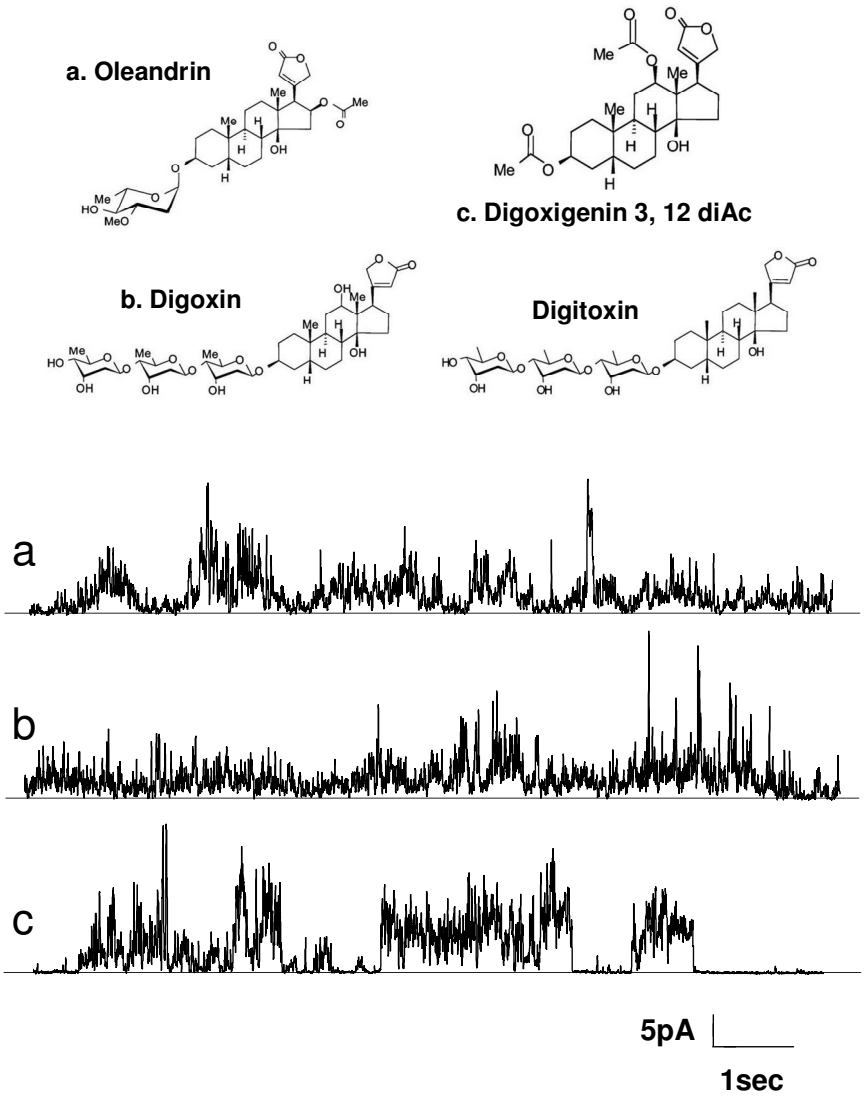

Figure 3

Fig. 13. Structures and activities of digitoxin-related cardiac glycosides. (*a*) Oleandrin forms digitoxin-like cation-specific channels in POPS/POPE planar lipid bilayers. (*b*) Digoxin forms digitoxin-like cation-specific channels in POPS/POPE planar lipid bilayers. (*c*) Digoxigenin 3,12-diAc forms digitoxin-like cation-specific channels in POPS/POPE planar lipid bilayers.

Concentration-Dependent Actions of Digitoxin

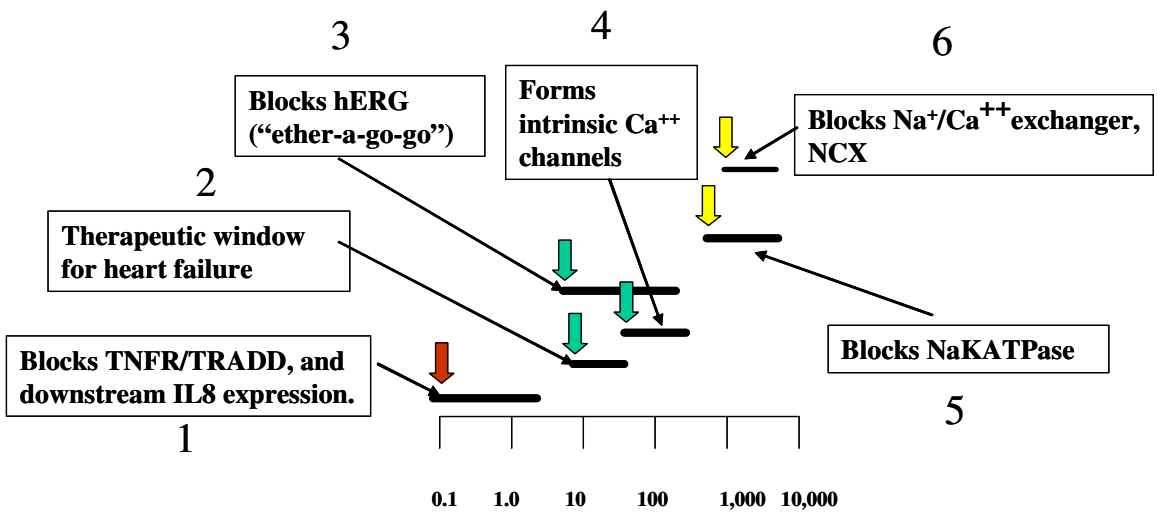

[Order of Activities: 1 > 2 >3 >4 >5 = 6]

Supplemental Figure 14. Summary of concentration dependent actions of digitoxin.

(**1**) In concentration range of 0.1-2.0 nM, digitoxin blocks the interaction between TNFR1 and TRADD, and downstream expression of IL-8. (**2**) The therapeutic window for heart failure is *ca.* 5-30 nM. (**3**) In range of 10-100 nM, digitoxin blocks hERG channel trafficking. (**4**) Above ca. 40 nM, digitoxin forms multimeric calcium channels. (**5**) In range of 300 nM and above, digitoxin and other active cardiac glycosides block the NaKATPase. (**6**) In the range of 3−20 μM, cardiac glycosides are said to block the Na^{+}/ Ca^{++} Exchanger (NCX) through primary action on the NaKATPase. Colored arrows discriminate between the three discrete clusters of functional activities.